JACS
JOURNAL OF THE AMERICAN CHEMICAL SOCIETY
COMMUNICATION
pubs.acs.org/JACS

ESI-MS Assay of *M. tuberculosis* Cell Wall Antigen 85 Enzymes Permits Substrate Profiling and Design of a Mechanism-Based Inhibitor

Conor S. Barry,[†] Keriann M. Backus,[†,§] Clifton E. Barry, III,[*,§] and Benjamin G. Davis[*,†]

[†]Department of Chemistry, University of Oxford, Chemistry Research Laboratory, Mansfield Road, Oxford OX1 3TA, U.K.
[§]Tuberculosis Research Section, Laboratory of Clinical Infectious Diseases, U.S. National Institute of Allergy and Infectious Disease, Bethesda, Maryland, United States

S Supporting Information

ABSTRACT: *Mycobacterium tuberculosis* Antigen 85 enzymes are vital to the integrity of the highly impermeable cell envelope and are potential therapeutic targets. Kinetic analysis using a label-free assay revealed both mechanistic details and a substrate profile that allowed the design and construction of a selective *in vitro* mechanism-based inhibitor.

Mycobacterium tuberculosis (*Mtb*), the causative agent of tuberculosis, is among the foremost causes of death and morbidity worldwide. It persists within the host with the aid of a complex and highly impermeable cell envelope containing a high content of long-chain fatty acids (mycolic acids) present as mycolate esters of arabino-galactan and of trehalose **1**.[1−3] Trehalose di- and monomycolates (TDM **2a** and TMM **3a**, respectively) are interconverted by the Antigen 85 a,b, and c (Ag85) mycolyltransferase isoforms (Figure 1).[4−6] The Ag85 enzymes play a vital role in the construction and maintenance of the cell envelope,[7] and have recently been shown to display plasticity for substrates based upon the trehalose motif.[8] Genetic 'knockouts' highlight Ag85c as the most active isoform; loss causes a 40% decrease in mycolate content of the cell wall.[9] These enzymes are therefore suggested targets for novel antimycobacterial drugs,[7] the development of which would benefit from a rapid and accurate assay of Ag85 activity and a thorough understanding of enzyme mechanism through the development of potential probes. However, despite the availability of several crystal structures and K_M estimates measured under pseudo-single-substrate conditions or with heterogeneous substrates, no detailed kinetic analysis or structure−activity relationship (SAR) studies have been reported. Current assays include nonspecific radiometric procedures for the detection of generic mycolyltransferase activity and coupled enzymatic assays for Ag85c.[4−6] Such methods preclude the possibility of readily automated screening or do not allow complete dissection of the steps of Ag85 acyl transfer, respectively. We report here the implementation of a label-free assay that allows full kinetic analysis as well as the potential for moderate-throughput screening; a panel of representative monosaccharides was used to map configurational structure−activity relationships. Together these data allowed the design of a mechanism-based inhibitor probe of Ag85c.

Mass spectrometry (MS) can be readily automated, and multiple natural substrates and products can be monitored simultaneously to give an unimpeded view of kinetic processes.[10−13] Kinetic analysis and substrate/inhibitor profiling were enabled by the development of a precise and quantitative MS assay of Ag85 activity based on total ion counts (TICs) of ions corresponding to trehalose, 6,6′-dihexanoyltrehalose **2b** (TDH), and 6-hexanoyltrehalose **3b** (TMH) (Figure 1). This exploited our previously described[11] calibration approach with a pseudointernal standard (here *N*-acetyl-D-glucosamine) injected concurrently with the sample aliquot; calibration plots for each monitored mass allowed quantitative measurements of concentration.

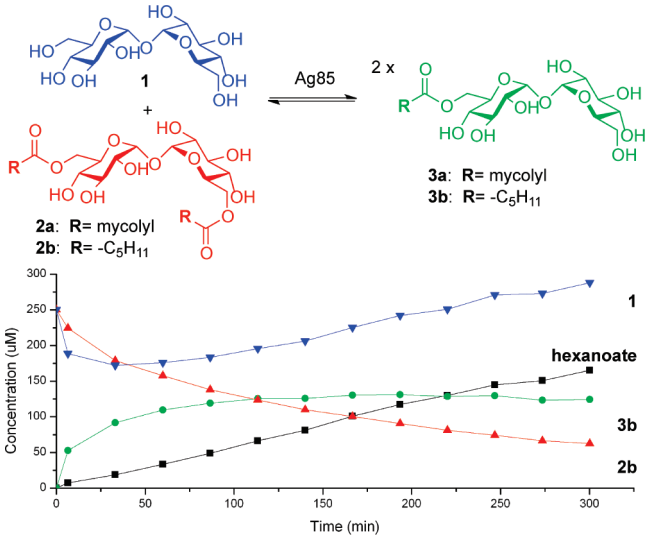

Figure 1. Reaction timecourse catalyzed by Ag85. *Conditions*: 250 μM **1**, 250 μM **2b**, 2 μM Ag85c, 1 mM TEA buffer (pH 7.2), 37 °C. Full kinetic analysis utilized the full range of conditions [Tre] = 5−125 μM, [**2b**] = 25−600 μM, [Ag85c] = 10 nM.

Full bi-substrate kinetic analysis was performed by determining initial rates of TMH **3b** formation at varied TDH **2b** and trehalose **1** concentrations.[10−13] These data were fitted by nonlinear regression methods to a range of plausible kinetic models, including modified rate equations that account for multiple acyl transfer pathways.[14] Together these and double-reciprocal analysis (see Supporting Information [SI]) ruled out simple (e.g., bi-bi ping-pong) mechanisms[15,16] that are typical of other

Received: May 9, 2011
Published: July 21, 2011

Table 1. Bi-substrate Kinetic Analysis of Ag85c

V_t (μM/min)	0.70 ± 0.05	$k_{cat\ (acyl\text{-}transfer)}$ (s^{-1})	1.16
V_h (μM/min)	0.29 ± 0.08	$k_{cat\ (hydrolysis)}$ (s^{-1})	0.49
$K_{M(TDH)}$ (μM)	266.8 ± 41.2	$k_{cat}/K_{M(TDH)}$ ($M^{-1}\ s^{-1}$)	4.35×10^3
$K_{M(Tre)}$ (μM)	16.9 ± 5.3	$k_{cat}/K_{M(Tre)}$ ($M^{-1}\ s^{-1}$)	6.88×10^4
$K_{i(TDH)}$ (μM)	355.3 ± 105.6		

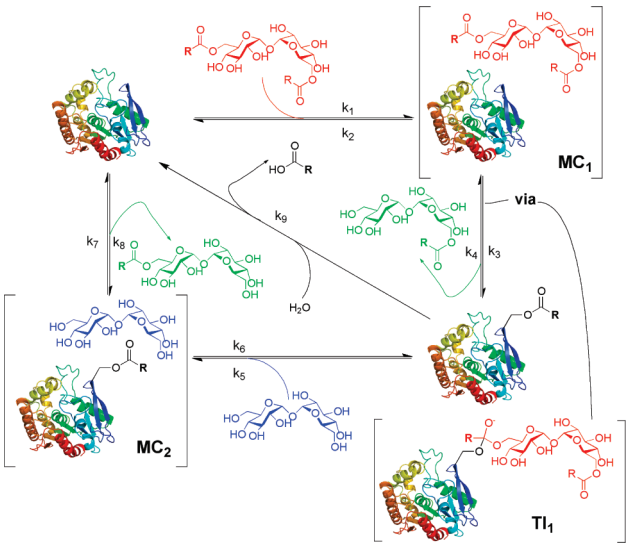

Figure 2. Mechanistic outline for Ag85.

acyltransferases. Nonetheless, crystal structure data show a clear Ser-His-Asp catalytic triad at the trehalose binding site of Ag85,[17] the serine of which has been mutated and nonspecifically modified, suggesting a role as a nucleophile;[18] it has also been reported that Ag85 can form a mycolyl−enzyme complex.[6]

Determination of the full kinetic parameters for Ag85c (Table 1) including K_M values for both substrates and separate maximal reaction velocities for acyl transfer (V_t) and hydrolysis (V_h), resolved this apparent conundrum and revealed considerable acylhydrolase activity (k_{cat} 0.49 s^{-1}) in contrast with prior reports.[6,19] We reasoned that this previously unreported activity of Ag85 was likely enzyme-mediated.[20] Indeed, analysis using a suitably modified ping-pong cycle gave an excellent correlation with the data ($R^2 > 0.99$). The implied mechanism (Figure 2) is therefore one of ping-pong formation of a hydrolytically unstable acyl enzyme intermediate that then releases catalyst through two competitive pathways. Although rare, such mechanisms are not entirely unprecedented.[21−23] This insight informed later inhibitor design (*vide infra*).

This precise dissection of different activities highlighted a strong advantage compared with, for example, single-substrate coupled assays that survey only one part of a given mechanistic cycle.[19] The value for $K_{M(Tre)}$ correlated well with the only previous value of 8.3 μM, determined under pseudo-single-substrate conditions.[6] A higher K_M value determined for TDH may reflect the homogeneous, shorter lipid chain of **2b** compared with heterogeneous mycolic acid substrates. The relative acyltransferase activities of the three Ag85 isoforms were also determined under pseudo-single-substrate conditions by monitoring the production of both TMH and hexanoate concurrently (Table 2), and confirmed the higher activity of Ag85c compared to those of Ag85a or Ag85b.[24]

Table 2. Kinetic Parameters for Ag85 Isoforms Recorded under Pseudo-Single-Substrate Conditions

Ag85 isoform	varied substrate[a]	K_M(app) (μM)	k_{cat}(app) (s^{-1})	k_{cat}(app)/K_M (app) ($M^{-1}\ s^{-1}$)
a	**1**	175	0.014	82
b	**1**	112	0.003	30
c	**1**	62	0.182	2952

[a] Assay conditions: [TDH] = 500 μM, [trehalose] = 10−250 μM, [Ag85a/b] = 500 nM, [Ag85c] = 50 nM.

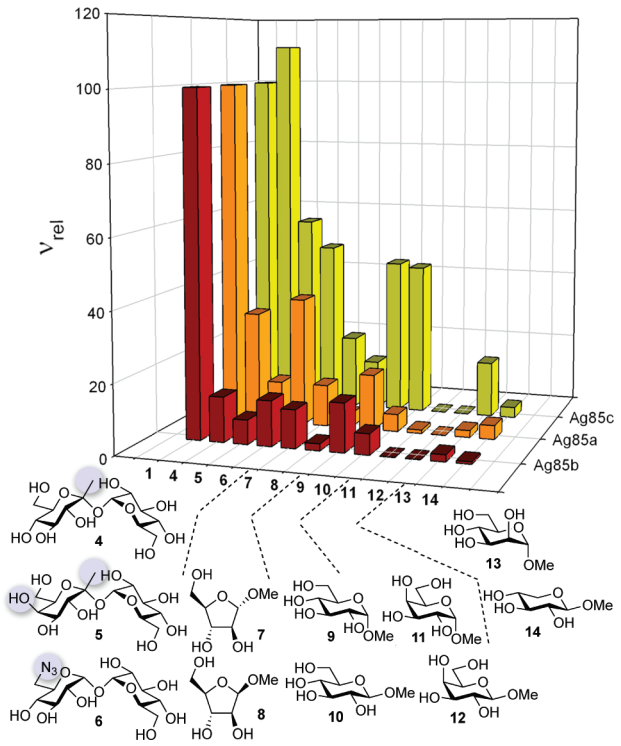

Figure 3. Substrate profiling screen and related compound structures. Assay conditions: 500 μM TDH, 500 μM screen compound, 2 μM Ag85 incubated at 37 °C for 160 min before measurement of v (product/substrate peak ratio). $v_{rel} = 100 \times (v/v_{Tre})$. See SI for Table S1.

With an accurate automated assay of Ag85 activity in place we then probed substrate selectivity. We have previously shown the utility of a semiquantititative green-amber-red (GAR) moderate-throughput screen to discover novel substrates for other bi-substrate (glycosyltransferase) enzymes.[10−13] Relative reaction velocity (v_{rel}) was determined by MS-based GAR assay for a panel of putative substrates (Figure 3, Table S1[SI]) to evaluate their suitability as acyl acceptors. Both trehalose (**1**) itself and related disaccharides **4** and **5** were found to act as substrates,[8] although the measured v_{rel} for **5** was lower for Ag85a and b, indicating the sensitivity of the enzymes to altering this scaffold configuration away from that found in trehalose (here through inversion at C-4). Interestingly, **6**, a known inhibitor of mycobacterial growth and previously described as an *in vitro* inhibitor of Ag85c activity is also a substrate for all Ag85 isoforms, indicating that it acts as a competitive substrate and suggesting that the observed antibacterial activity may arise from downstream events after Ag85-mediated mycolyltransfer or through inhibition of other pathways.[4,25]

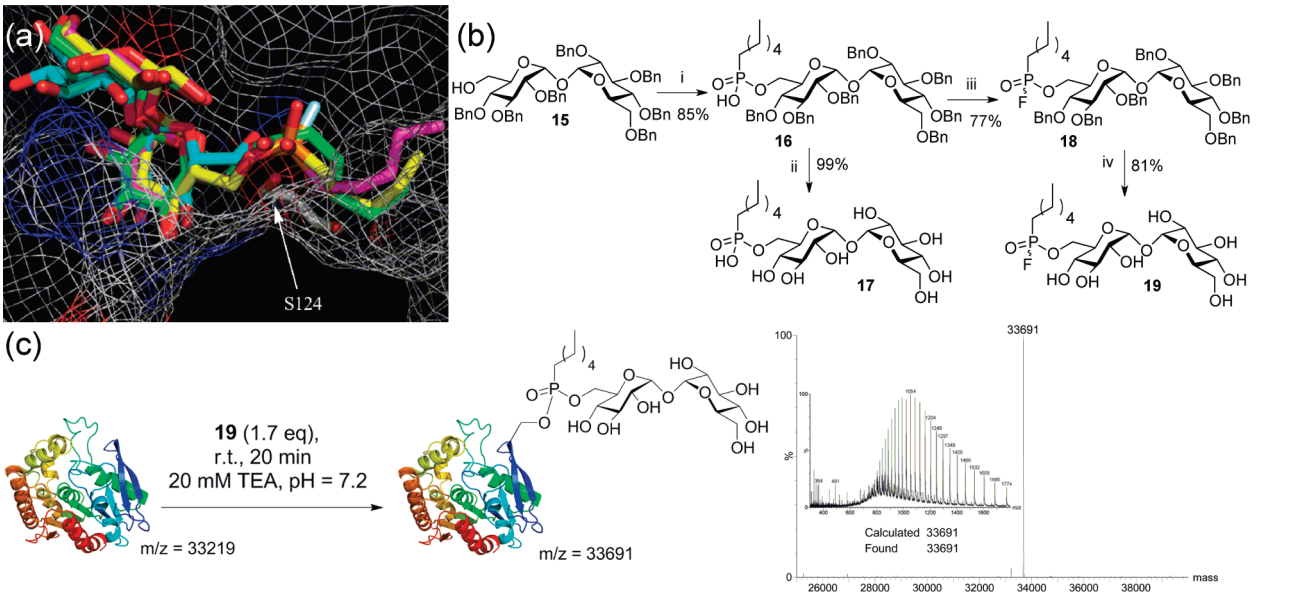

Figure 4. Synthesis and evaluation of probe **19**. (a) Lowest energy binding poses in the active site of Ag85c of trehalose **1** (cyan), TMH **2b** (green), **17** (yellow) and **19** (magenta). The active site serine is shown with an arrow. Image produced using PyMol,[26] and docking poses generated with AutoDock Vina[27] from pdb 1DQZ. (b) Synthesis of inhibitors **17** and **19**. *Reagents and conditions*: i) hexyldichlorophosphate, pyridine, rt, 16 h; ii) 1:1 EtOH/H_2O, Pd−C, H_2, rt, 18 h; iii) BTFFH, DIPEA, DMF, rt, 18 h; iv) 1:1 EtOH/H_2O, Pd−C, H_2, rt, 18 h. (c) Reaction of probe **19** with Ag85c indicates essentially complete conversion to covalently modified Ser124 adduct by ES-MS.

Despite observed plasticity for variants of the trehalose scaffold, truncated or more dramatically altered sugar variants displayed considerably lower activity. Although trehalose is a 1, 1-diglucoside, methyl D-glucosides **9** and **10** were utilized less efficiently. Interestingly, some low-level activity (up to ∼20%) was also observed for the arabinofuranosides **7** and **8**; this is consistent with a possible role of Ag85 in mycolate scrambling and mycolation of *Mtb* arabinogalactan. Notably, for these glucosides and arabinosides differential anomeric selectivity between enzyme isoforms was observed: α-anomers were preferred by Ag85a and b, with Ag85c showing little anomer discrimination. In keeping with this observation of tolerance at the anomeric center, Ag85c also showed the greatest tolerance toward ketosides **4** and **5**, which carry an additional methyl substituent at C-1. As for the disaccharides, configurational changes had a more dramatic effect. The very low v_{rel} value determined for D-galactosides **11** and **12** for all three Ag85 isoforms is clear additional evidence that the epimeric configuration at C-4 is a crucial selectivity determinant. Conversely, α-methyl mannoside **13** was slowly utilized by Ag85c, indicating some degree of flexibility with respect to C-2 configuration. As expected, xyloside **14** was also poorly processed, confirming that the majority of acyl transfer is OH-6. These differences in substrate recognition stand in contrast to the conserved active site of these three isoforms and suggest that the enzymes may well have distinct physiological roles.[18]

With this understanding of substrate tolerance, we sought to rationally design an effective covalent inhibitor probe. Although nonspecific approaches based simply on serine modification might be considered,[18] the true utility of this probe would be vitally dependent on selectivity. Design was therefore essentially informed by both mechanism (Figure 2) as well as by the substrate screen. These dictated an inhibitor structure that would mimic the tetrahedral intermediate (TI) formed in the first unified 'ping-to-pong' acylation steps rather than through intervention in the divergent pathways for deacylation (Figure 2). Fluorophosphonate **19** (Figure 4b) was therefore based upon (a) targeting the TI of acylation (**TI_1**) through the *in situ* formation of a tetrahedral mimic (Figure 2);[28] (b) targeting of the same TI by ensuring features that also mimic both lipid and sugar moieties (Figure 2); (c) substrate preferences that highlight trehalose as a superior sugar scaffold (Figure 3). *In silico* evaluation supported another aspect of design with these features: molecular docking[27] was performed to compare binding modes that would correspond to putative Michaelis complexes (Figure 2, **MC_1** and Figure 4a). Lowest energy conformations of **19** (−7.3 kcal mol^{-1}) overlaid closely with both TMH **2b** (−7.0 kcal mol^{-1}) and also with trehalose (observed in the crystal structure of Ag85b, pdb: 1F0P[17]), placing the acyl carbon (in **2b**) and phosphoryl phosphorus (in **19**) in close proximity to the targeted active site serine 124.

19 was readily synthesized from hepta-benzyl-trehalose **15**[8] (Figure 4b). Treatment of **16** with fluoro-*N,N,N′,N′*-bis-(tetramethylene)formamidinium hexafluorophosphate (BTFFH) afforded **18** in good yield; deprotection by catalytic hydrogenolysis gave **19** with no concomitant hydrolysis of the phosphorylfluoride.

The inhibitory potential of **19** against Ag85c was assayed using a saturating concentration of trehalose (>25× K_M) to ensure maximal turnover rate. Following incubation of Ag85c with **19** (150μM) activity was almost entirely ablated (<7%). Phosphonate **17**, an unreactive analogue of **19** that cannot effectively mimic the targeted TI resulted in inhibition only to 46%.[29] k_{obs}/K_i was determined to be 1420 (±90) min^{-1} mM^{-1} (see SI); the reactivity of **19** is such that saturation could not be achieved, as has been reported for other covalent inhibitors.[30] This marks **19** as a potent inhibitor in comparison with other fluorophosphonates.[31,32] With inhibitory potential confirmed, critical selectivity of **19** for Ag85 over other enzymes that contain similar catalytic triads was investigated. Serine protease subtilisin from *Bacillus lentus* (SBL), lipase B from *Candida antarctica* (CalB),

and Ag85c were incubated under identical conditions with **19**. Detailed analysis by MS revealed essentially complete protein modification of Ag85c at Ser124 (Figure 4c and SI), while no detectable modification or inhibition of either SBL or CalB was observed.

MS has provided an accurate and automated method to determine the full kinetic parameters of Ag85c, which revealed that the enzyme displays a combination of acyltransferase and acylhydrolase activities. Substrate profiling revealed that, although the Ag85 enzymes show promiscuity for trehalose-based substrates,[8] selectivity for differing monosaccharides and anomeric configurations is marked: gluco- and arabinofuranosides are preferred over galacto-, manno-, or xylopyranosides. These data provide additional evidence that Ag85 is responsible for both trehalose−mycolate scrambling and mycolylation of the mycobacterial arabinogalactan. They also suggest that regions distal to the active sites influence activity of the three isoforms. The screen data indicate that disaccharides are better substrates than the constituent monosaccharides, which suggests an extended active site. This in turn suggests that the optimal starting point for rational drug design may be the trehalose scaffold that was used here to design a tailored fluorophosphonate **19**. This compound was a potent and highly selective covalent inhibitor probe of Ag85c that shows no reactivity toward other serine acyltransferases. The selectivity of this molecule may allow interrogation of the importance of Ag85 activity in vitro or in infected macrophages. We anticipate that this and related 'tagged' compounds may find use as activity-based probes[33] of Ag85 function and might serve as a starting point for the design of novel anti-mycobacterial drugs.

■ ASSOCIATED CONTENT

Supporting Information. Experimental methods and supporting figures. This material is available free of charge via the Internet at http://pubs.acs.org.

■ AUTHOR INFORMATION

Corresponding Author
cbarry@niaid.nih.gov; Ben.Davis@chem.ox.ac.uk

■ ACKNOWLEDGMENT

This work was funded by the Intramural Research Program of the National Institutes of Health, National Institute of Allergy and Infectious Disease (C.E.B.), the Rhodes Trust (K.M.B.), the Biotechnology and Biological Sciences Research Council (C.S.B.), and the Bill and Melinda Gates Foundation through the TB Drug Accelerator Program (C.E.B, B.G.D.). B.G.D. is a Royal Society Wolfson Research Merit Award recipient. We thank Colorado State "TB Vaccine Testing and Research Materials" contract for providing Antigen 85 plasmids.

■ REFERENCES

(1) Brennan, P. J.; Nikaido, H. *Annu. Rev. Biochem.* **1995**, *64*, 29–63.
(2) Draper, P.; Daffe, M. In *Tuberculosis and the Tubercle Bacillus*; ASM Press: Washington DC, 2005.
(3) Mills, J. A.; Motichka, K.; Jucker, M.; Wu, H. P.; Uhlik, B. C.; Stern, R. J.; Scherman, M. S.; Vissa, V. D.; Pan, F.; Kundu, M.; Ma, Y. F.; McNeil, M. *J. Biol. Chem.* **2004**, *279*, 43540–43546.
(4) Belisle, J. T.; Vissa, V. D.; Sievert, T.; Takayama, K.; Brennan, P. J.; Besra, G. S. *Science* **1997**, *276*, 1420–1422.
(5) Kilburn, J. O.; Takayama, K.; Armstrong, E. L. *Biochem. Biophys. Res. Commun.* **1982**, *108*, 132–139.
(6) Sathyamoorthy, N.; Takayama, K. *J. Biol. Chem.* **1987**, *262*, 13417–13423.
(7) Chatterjee, D. *Curr. Opin. Chem. Biol.* **1997**, *1*, 579–588.
(8) Backus, K. M.; Boshoff, H. I.; Barry, C. S.; Boutureira, O.; Patel, M. K.; D'Hooge, F.; Lee, S. S.; Via, L. E.; Tahlan, K.; Barry, C. E., III; Davis, B. G. *Nat. Chem. Biol.* **2011**, *7*, 228.
(9) Jackson, M.; Raynaud, C.; Laneelle, M. A.; Guilhot, C.; Laurent-Winter, C.; Ensergueix, D.; Gicquel, B.; Daffe, M. *Mol. Microbiol.* **1999**, *31*, 1573–1587.
(10) Flint, J.; Taylor, E.; Yang, M.; Bolam, D. N.; Tailford, L. E.; Martinez-Fleites, C.; Dodson, E. J.; Davis, B. G.; Gilbert, H. J.; Davies, G. J. *Nat. Struct. Mol. Biol.* **2005**, *12*, 608–614.
(11) Yang, M.; Brazier, M.; Edwards, R.; Davis, B. G. *ChemBioChem* **2005**, *6*, 346–357.
(12) Yang, M.; Davies, G. J.; Davis, B. G. *Angew. Chem., Int. Ed.* **2007**, *46*, 3885–3888.
(13) Yang, M.; Proctor, M. R.; Bolam, D. N.; Errey, J. C.; Field, R. A.; Gilbert, H. J.; Davis, B. G. *J. Am. Chem. Soc.* **2005**, *127*, 9336–9337.
(14) See SI for derivation.
(15) See SI for details of double reciprocal analysis of Ag85c.
(16) Cook, P. F.; Cleland, W. W. *Enzyme Kinetics and Mechanism*; Garland Science: London; Abingdon, 2007.
(17) Anderson, D. H.; Harth, G.; Horwitz, M. A.; Eisenberg, D. *J. Mol. Biol.* **2001**, *307*, 671–681.
(18) Ronning, D. R.; Klabunde, T.; Besra, G. S.; Vissa, V. D.; Belisle, J. T.; Sacchettini, J. C. *Nat. Struct. Biol.* **2000**, *7*, 141–146.
(19) Boucau, J.; Sanki, A. K.; Voss, B. J.; Sucheck, S. J.; Ronning, D. R. *Anal. Biochem.* **2009**, *385*, 120–127.
(20) Cook, P. F.; Tai, C. H.; Hwang, C. C.; Woehl, E. U.; Dunn, M. F.; Schnackerz, K. D. *J. Biol. Chem.* **1996**, *271*, 25842–25849.
(21) Brown, A. J.; Snyder, F. *J. Biol. Chem.* **1982**, *257*, 8835–8839.
(22) Casals, C.; Acebal, C.; Arche, R. *Int. J. Biochem.* **1984**, *16*, 773–778.
(23) The divergent deacylation pathways may also be related to the nature/identity of the fatty acyl chain.
(24) $\nu_{\text{transfer}} = (\nu_{\text{TMH}} - \nu_{\text{hydrolysis}})/2$
(25) Kalscheuer, R.; Syson, K.; Veeraraghavan, U.; Weinrick, B.; Biermann, K. E.; Liu, Z.; Sacchettini, J. C.; Besra, G.; Bornemann, S.; Jacobs, W. R. *Nat. Chem. Biol.* **2010**, *6*, 376–384.
(26) *The PyMOL Molecular Graphics System*, Version 0.99rc6: Schrödinger, LLC: http://pymol.org/pymol.
(27) Trott, O.; Olson, A. J. *J. Comput. Chem.* **2010**, *31*, 455–461.
(28) Bachovchin, D. A.; Ji, T. Y.; Li, W. W.; Simon, G. M.; Blankman, J. L.; Adibekian, A.; Hoover, H.; Niessen, S.; Cravatt, B. F. *Proc. Natl Acad. Sci. U.S.A.* **2010**, *107*, 20941–20946.
(29) See SI for details.
(30) McCarter, J. D.; Withers, S. G. *J. Am. Chem. Soc.* **1996**, *118*, 241–242.
(31) Diisopropylfluorophosphonate and soman have $k_{\text{obs}}/K_{\text{i}}$ values of 140 and 9200 $\text{min}^{-1}\ \text{mM}^{-1}$, respectively, against human acetylcholine esterase.
(32) Worek, F.; Thiermann, H.; Szinicz, L.; Eyer, P. *Biochem. Pharmacol.* **2004**, *68*, 2237–2248.
(33) Evans, M. J.; Cravatt, B. F. *Chem. Rev.* **2006**, *106*, 3279–3301.